Electronic Supplementary Information For

Achieving Biosensing at Attomolar Concentrations of Cardiac Troponin T in Human Biofluids by Developing a Label-Free Nanoplasmonic Analytical Assay

Thakshila Liyanage, Andeep Sangha, and Rajesh Sardar*

Department of Chemistry and Chemical Biology, Indiana University-Purdue University Indianapolis, 402 N. Blackford Street, Indianapolis, Indiana 46202, United States

*Email: rsardar@iupui.edu; Phone: 317-278-2511

Spectroscopy and Microscopy Characterization. A Varian Cary 50 Scan UV-visible spectrophotometer was used to collect absorption and extinction spectra in the range of 300-1100 nm. Absorption spectra of gold nanoprism solutions were obtained by diluting 0.3 mL of reaction solution to a final volume of 2.0 mL with acetonitrile in a 1 cm quartz cuvette. Acetonitrile was used as a background in each run before collecting the absorbance spectra. Background subtracted (using silanized glass coverslips) extinction spectra of our LSPR cTnT biosensors were measured in PBS buffer (pH 7.4) at room temperature. Before each measurement, the sensors were incubated in buffer solution for 10 min to equilibrate and then extinction spectra were collected. Scanning Electron Microscopy (SEM) was used to determine the average edge-length of gold nanoprisms used in our biosensors fabrication.

Synthesis of Gold Nanoprisms: We synthesized gold triangular nanoprisms (Au TNPs) according to our published method with minor modifications.[1,2] Briefly, $Et_3PAu(I)Cl$ (0.008 g, 0.02 mmol) was dissolved in 10 mL of acetonitrile and stirred for 5 min at room temperature followed by addition of a mixture of 0.085 mL of TOA and 0.3 mL of PMHS. Then the reaction mixture was gradually heated to 40 ^{o}C. During this time the color of the solution changed from colorless to pink, purple, and then blue. When the solution turned light blue, 9 mL acetonitrile was added to the reaction mixture and the Au TNP formation was allowed to proceed at this temperature. The reaction mixture was monitored through UV-visible absorption spectroscopy to follow the dipole peak position (λ_{LSPR}) of Au TNPs. The reaction mixture was removed from heat once the desired λ_{LSPR} peak was reached, e.g., 760, 800, and 820 nm in acetonitrile (Figure S1), which represent average edge-lengths of 34, 42, and 47, respectively.[1-4] The sizes were confirmed by SEM analysis.

Silanization of Glass Coverslips: Glass coverslips were functionalized based on our published procedure.[1,2] As a first step, coverslips were incubated in a RBS 35 detergent solution at 90 ^{o}C for 10 min in a sonicator. The coverslips were then thoroughly rinsed with nanopure water and further incubated in a solution containing concentrated hydrochloric acid and methanol (1:1 v/v) for 30 min. Finally, coverslips were rinsed with nanopure water and placed in a vacuum oven at 60 ^{o}C overnight. Next the cleaned coverslips were immersed in a 10% MPTES solution in ethanol for 30 min, and then sonicated for 10 min followed by rinsing with ethanol. Finally, MPTES-functionalized coverslips were dried in a vacuum oven at 120 ^{o}C for 3 h.

LOD and K_D Calculations. The LODs were determined according to the literature as follows: (1) Measure the $\Delta\lambda_{LSPR}$ for the blank sample (anti-cTnT functionalized Au TNPs attached onto glass coverslips). (2) Determine the *Z* (mean + 3σ) value, where σ is the standard deviation.[5] (3) Convert *Z* value into relative concentration using a calibration curve. We determined the effective dissociation constant (K_D) using the highest $\Delta\lambda_{LSPR}$ value and then best fit the data to a Langmuir isotherm.[6]

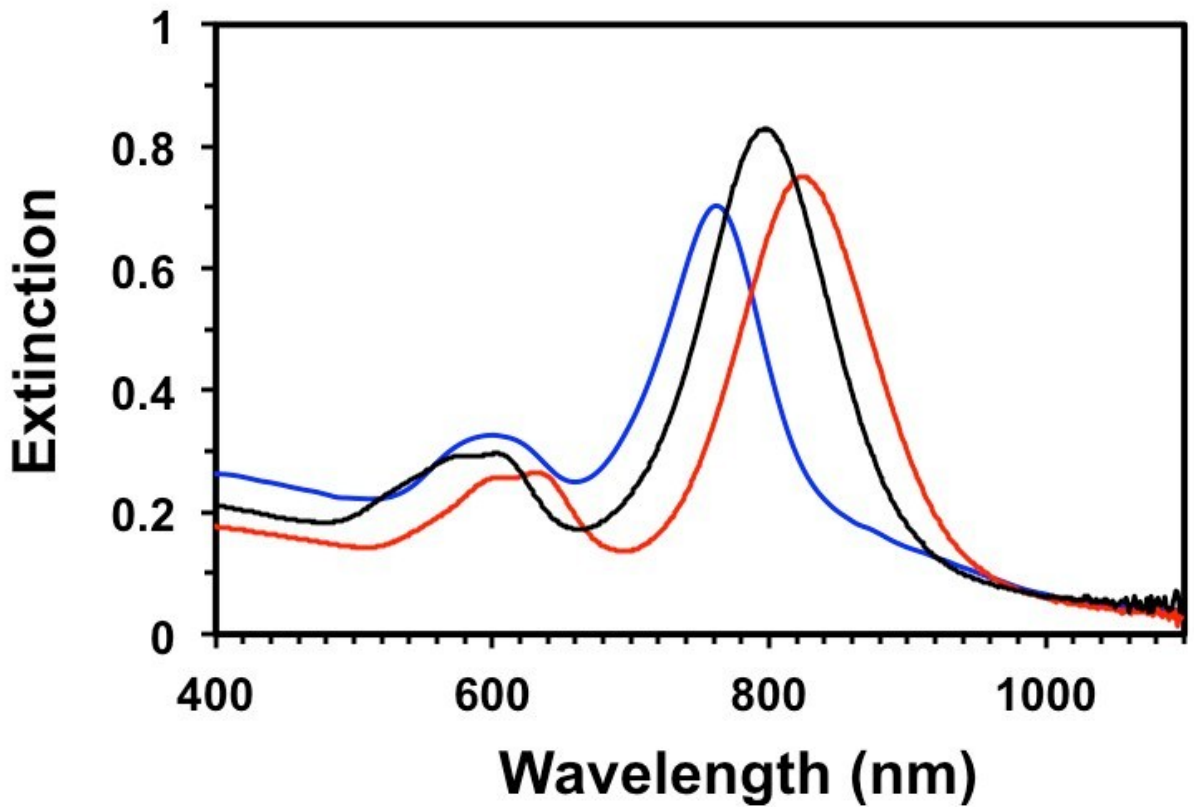

Fig. S1. UV-visible absorption spectra of Au TNPs in acetonitrile. LSPR dipole peaks ($\lambda_{LSPR, dipole}$) are as follows: 750 nm with edge-length 34 nm (blue), 800 nm with edge-length 42 nm (black), and 825 nm with edge-length 47 nm (red).

Table S1. Calibration curve and the limit of detection (LOD) for chip-based LSPR cTnT sensors constructed with various edge lengths of Au TNPs.

λ_{LSPR} (nm)[a]	Edge Length (S.D)[b,c]	Equation	Z value (nm)	R^2 Value	LOD (ng/L)	LOD (pM)
750	34 (2.6)	y = 0.391ln(x) - 0.389	2.3	0.99	974	27.8
800	42 (3.5)	y = 0.598ln(x) - 0.888	1.7	0.98	75.4	2.2
820	47 (4.9)	y = 0.503ln(x) + 1.628	1.6	0.98	0.9	0.026

[a]The LSPR dipole peak position (λ_{LSPR}) of Au TNPs in acetonitrile. [b]S.D. represents standard deviation. [c]At least 500 Au TNPs from two different synthesis batches were counted to determine the average edge-length.

Table S2. $\Delta\lambda_{LSPR}$ responses from cTnT sensors, which were constructed with three different edge length of Au TNPs in PBS buffer. Our current laboratory protocol is to fabricate at least five independent cTnT biosensors (n = 5) from two different batches of Au TNPs to determine the average $\Delta\lambda_{LSPR}$.

Au TNPs Edge-Length (nm)	cTnT Concentration (ng/L)	Average $\Delta\lambda_{LSPR}$	Standard Deviation (nm)
34	350000	4.5	0.6
	35000	3.8	0.5
	3500	2.9	0.5
	350	1.8	0.6
42	350000	6.6	0.4
	35000	5.8	0.4
	17500	4.9	0.5
	3500	3.8	0.2
	350	2.4	0.6
	35	1.4	0.4
47	350000	8.4	1.0
	35000	6.9	0.6
	3500	5.4	0.4
	350	4.3	0.5
	35	3.3	0.5
	3.5	2.4	0.6
	0.35	1.3	0.4

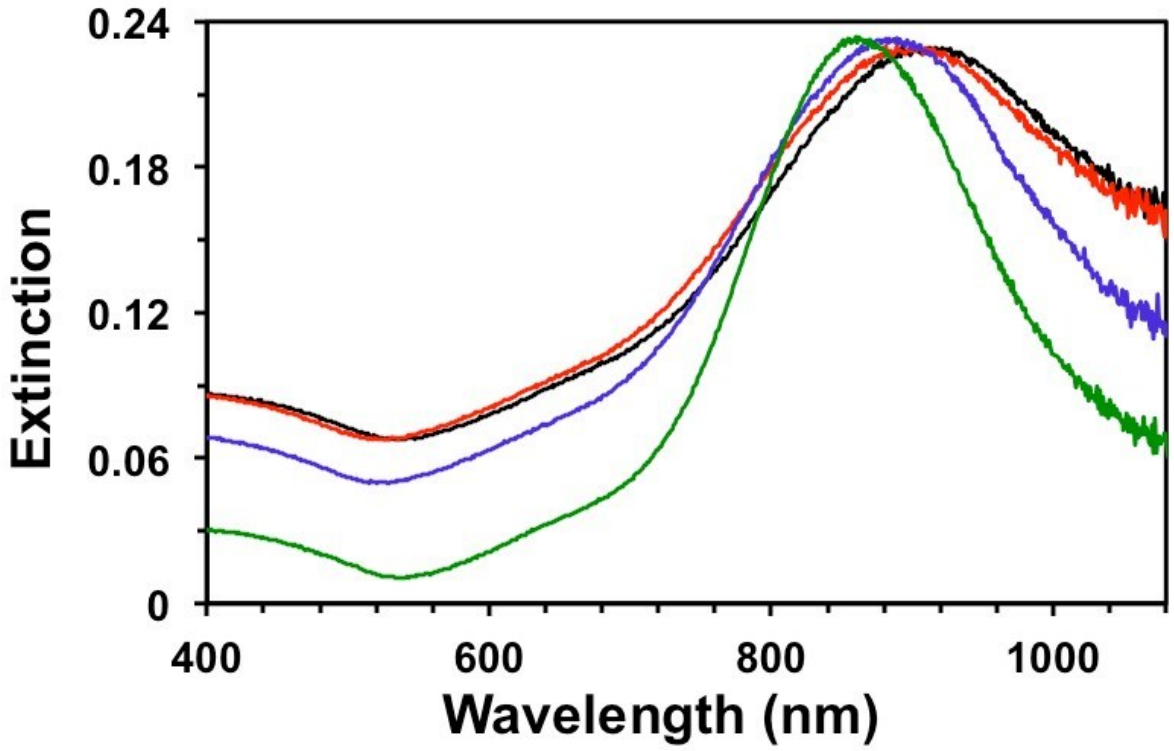

Fig. S2. Extinction spectra of 47 nm edge-length Au TNPs attach onto silanized glass substrate (green, λ_{LSPR} = 864 nm), after functionalization with 1:1 mole ratio of 1 mM solution of MHDA/DDT SAMs (blue, λ_{LSPR} = 891 nm), attachment of anti-cTnT through EDC/NHS coupling (red, λ_{LSPR} = 907 nm), and after incubation in 350000 ng/L (10 nM) of cTnT (black λ_{LSPR} = 915 nm). All spectra were collected in PBS buffer.

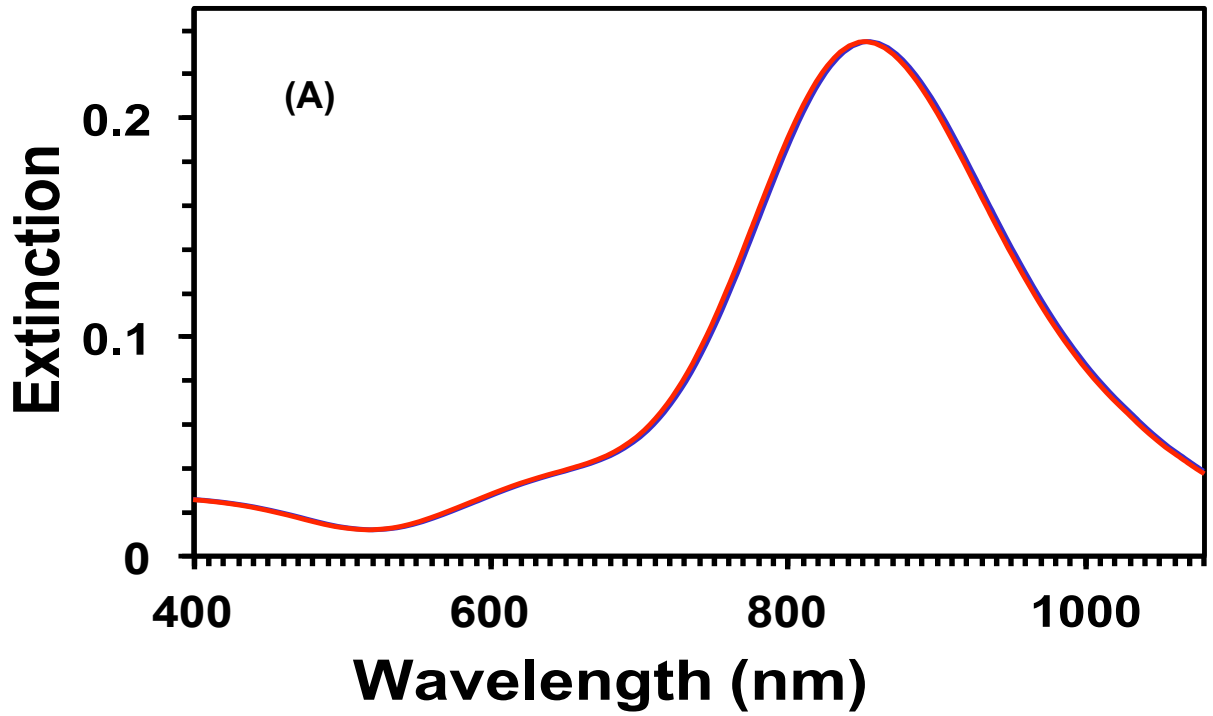
(A)
Extinction
0.2
0.1
0
400
600
800
1000
Wavelength (nm)

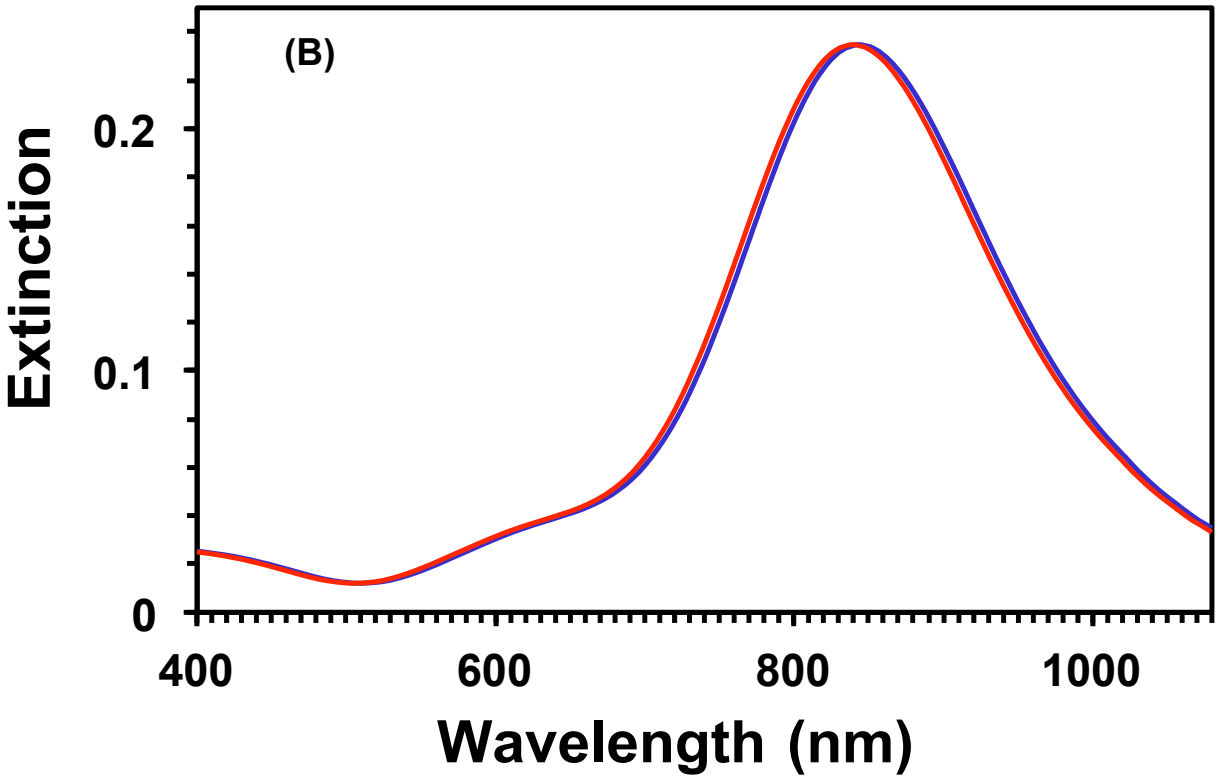
(B)
Extinction
0.2
0.1
0
400
600
800
1000
Wavelength (nm)

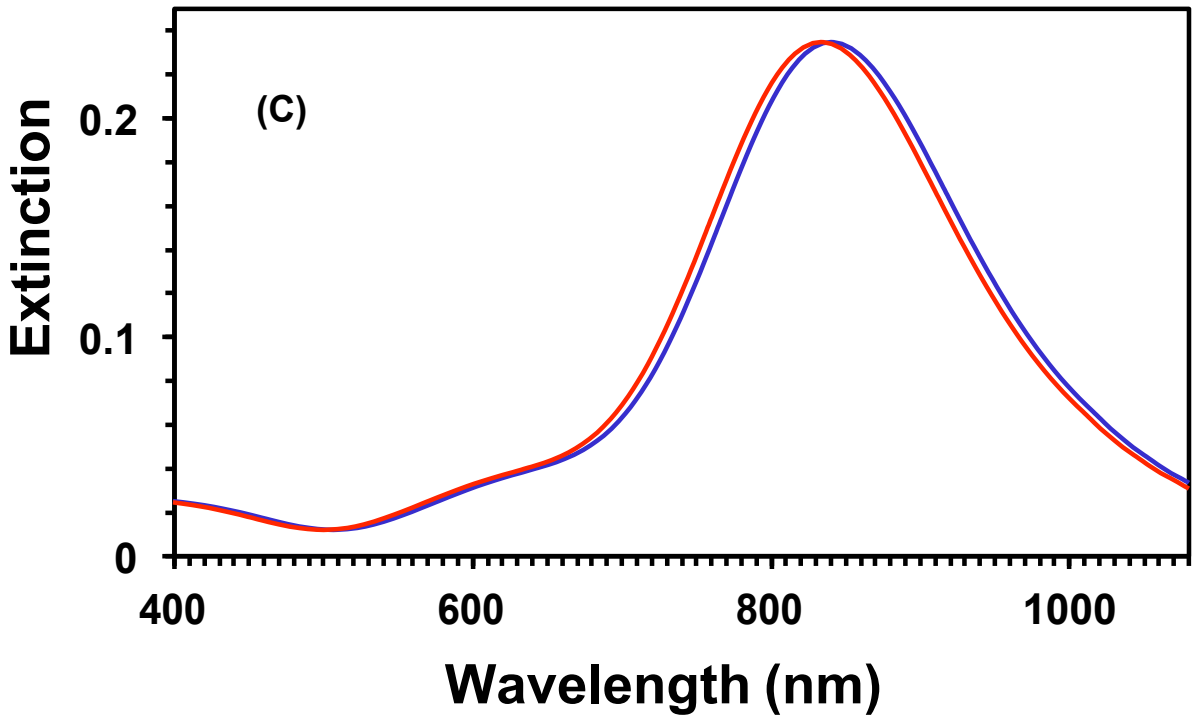

Fig. S3. Extinction spectra of chip-based LSPR cTnT sensors constructed with three different electromagnetic-field decay lengths by varying the carbon chain length of the alkylthiol SAMs (A) MHDA/DDT, (B) MUDA/NT, and (C) MHNA/HT before (red curves) and after (blue curves) incubation in 350 ng/L cTnT solution in PBS buffer. Red highlighted text in **Table S4** shows actual $\Delta\lambda_{LSPR}$ responses. All spectra were collected in PBS buffer.

Table S3. LOD derived for chip-based LSPR cTnT sensors constructed with three different type of SAMs while keeping the edge-length of Au TNPs constant.

Edge Length (nm)	SAM type	Equation	R^2 Value	Z value	LOD (ng/L)	LOD (pM)
42	MHDA/DDT	y = 0.598ln(x) - 0.888	0.98	1.7	75.4	2.2
42	MUDA/NT	y = 0.937ln(x) - 1.472	0.98	1.2	17.3	0.5
42	MHNA/HT	y = 0.548ln(x) + 3.529	0.94	2.2	0.1	0.003

Table S4. $\Delta\lambda_{LSPR}$ responses from cTnT sensors, which were constructed with three different SAMs in PBS buffer using 42 nm edge-length Au TNPs. Our current laboratory protocol is to fabricate at least five independent cTnT biosensors (n = 5) from two different batches of Au TNPs to determine the average $\Delta\lambda_{LSPR}$.

Edge Length (nm)	SAM type	cTnT Concentration (ng/L)	Average $\Delta\lambda_{LSPR}$ (nm)	Standard Deviation (nm)
42	MHDA/DDT	350000	6.6	0.4
		35000	5.8	0.4
		17500	4.9	0.5
		3500	3.8	0.2
		350	2.4	0.6
		35	1.4	0.4
42	MUDA/NT	350000	11.0	1.3
		175000	9.6	1.0
		35000	8.2	1.3
		17500	7.0	0.9
		3500	6.6	0.5
		1750	5.5	0.7
		350	4.3	0.5
		175	3.4	0.4
		35	1.7	0.4
42	MHNA/HT	1750	8.5	1.6
		350	6.8	1.0
		175	5.5	1.5
		35	5.0	1.4
		3.5	4.4	1.1
		1.75	3.8	1.7
		0.35	2.9	1.0
		0.035	2.0	0.8

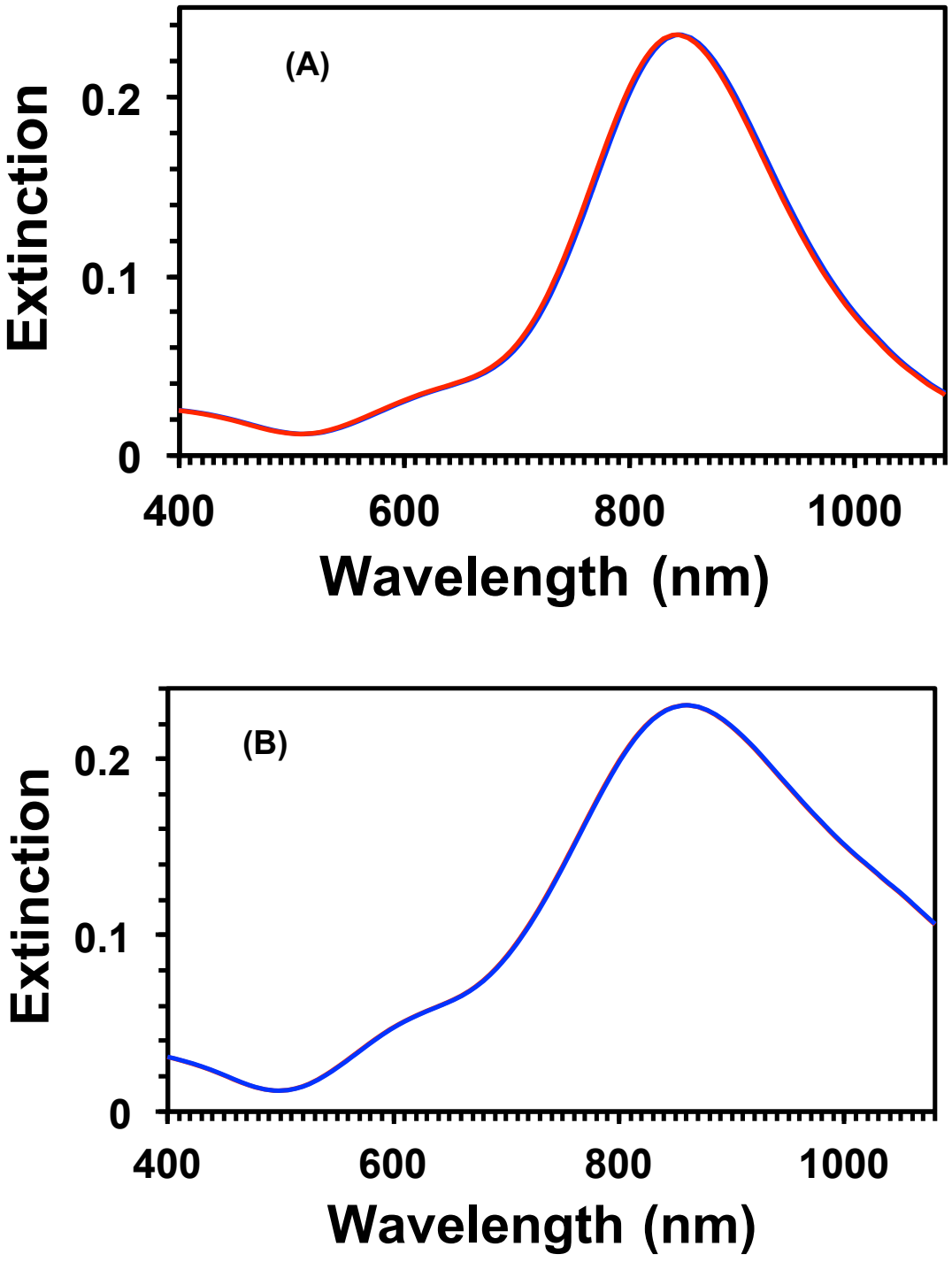

Fig. S4. Extinction spectra of just (A) MHNA/HT and (B) MUDA/NT SAM-modified Au TNPs attached onto silanized glass substrates (red curves) and after incubation in 35 ng/L cTnT in PBS buffer (blue curves). Due to exact spectral overlap, the red curve is not visible in the bottom spectra.

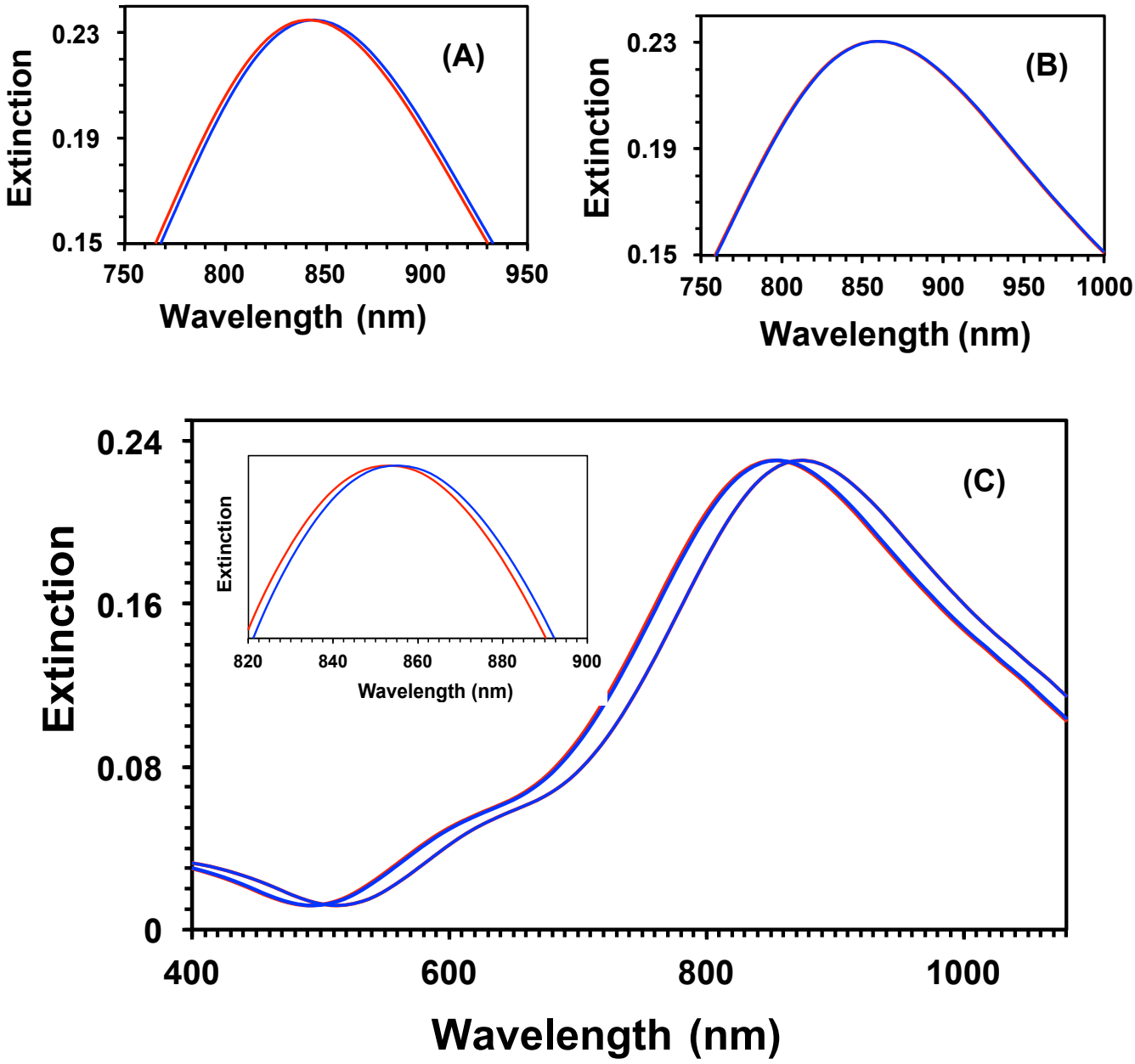

Fig. S5. Characterization of selectivity of LSPR cTnT biosensors. Expanded version of extinction spectra of MHNA/HT (A) and MUDA/NT (B) SAM-modified Au TNPs attached onto glass substrate before (red) and after incubation in 35 ng/L cTnT in PBS buffer. Because of spectral overlap, the red line in panel B is not clearly visible. (C) Extinction spectra of LSPR biosensors prepared with MHNA/HT (solid lines) and MUDA/NT (dashed lines) SAMs functionalized with anti-cTnT before (red) and after (blue) incubation with 35 ng/L tropomyosin in PBS buffer. The inset shows the expanded region of the spectra for a MHNA/HT SAM-containing cTnT sensor.

Table S5. $\square\lambda_{LSPR}$ responses from chip-based LSPR cTnT sensors fabricated by using MUDA/NT SAM of varied ratio. Our current laboratory protocol is to fabricate at least five independent cTnT biosensors (n = 5) from two different batches of Au TNPs to determine the average $\square\lambda_{LSPR}$.

cTnT Concentration (ng/L)	MUDA/NT ratio	Average $\square\lambda_{LSPR}$ (nm)	Standard Deviation (nm)
1750	5:5	5.5	0.7
	6:4	7.0	0.6
	7:3	9.2	0.7
	8:2	11.5	0.7

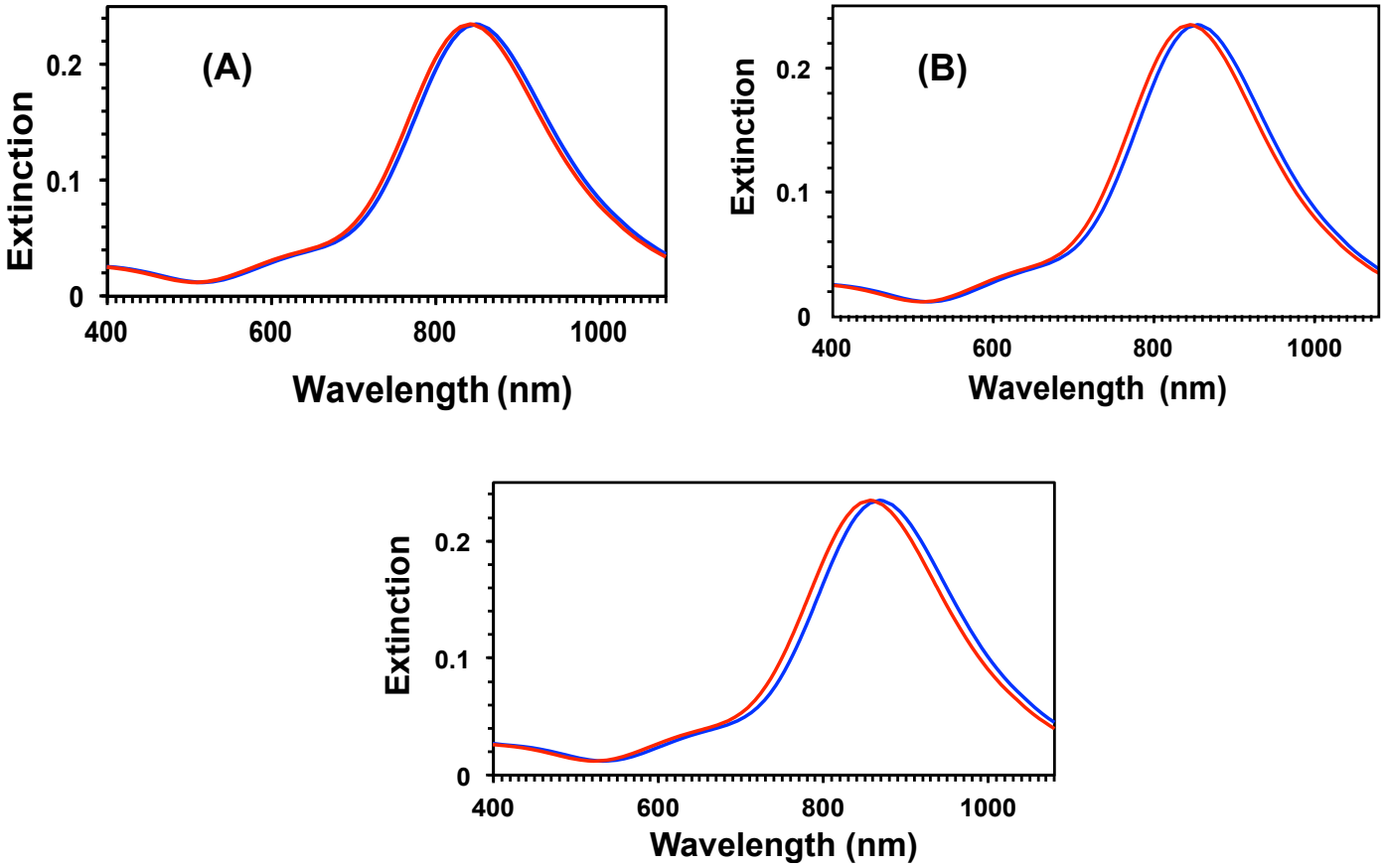

Fig. S6. Extinction spectra of chip-based LSPR cTnT sensors constructed with three different MUDA:NT ratios: (A) 6:4, (B) 7:3, and (C) 8:2. The red and blue curves represent before and after incubation of the sensors in 1750 ng/L cTnT PBS buffer. Table S5 shows actual $\square\lambda_{LSPR}$ responses.

Table S6. LOD of chip-based LSPR cTnT sensors fabricated using three different type of SAMs while keeping the edge-length of Au TNPs constant.[a]

Physiological Media	Equation	R^2 Value	Z Value (nm)	LOD* 10^{-6} (ng/L)	LOD
Buffer	y = 0.671ln(x) + 6.761	R^2 = 0.99	1.2	251	7.2
Buffer	y = 0.591ln(x) + 6.888	R^2 = 0.98	1.4	190	5.8
Plasma	y = 0.615ln(x) + 6.224	R^2 = 0.98	1.5	507	14.5
Plasma	y = 0.587ln(x) + 5.973	R^2 = 0.97	1.5	460	13.1
Serum	y = 0.624ln(x) + 5.676	R^2 = 0.98	1.2	766	21.9
Urine	y = 0.707ln(x) + 3.506	R^2 = 0.98	1.6	67360	1900

[a]Red (initially constructed calibration curve) and blue (calibration curve constructed after nearly 8 months) using our chip-based cTnT sensors.

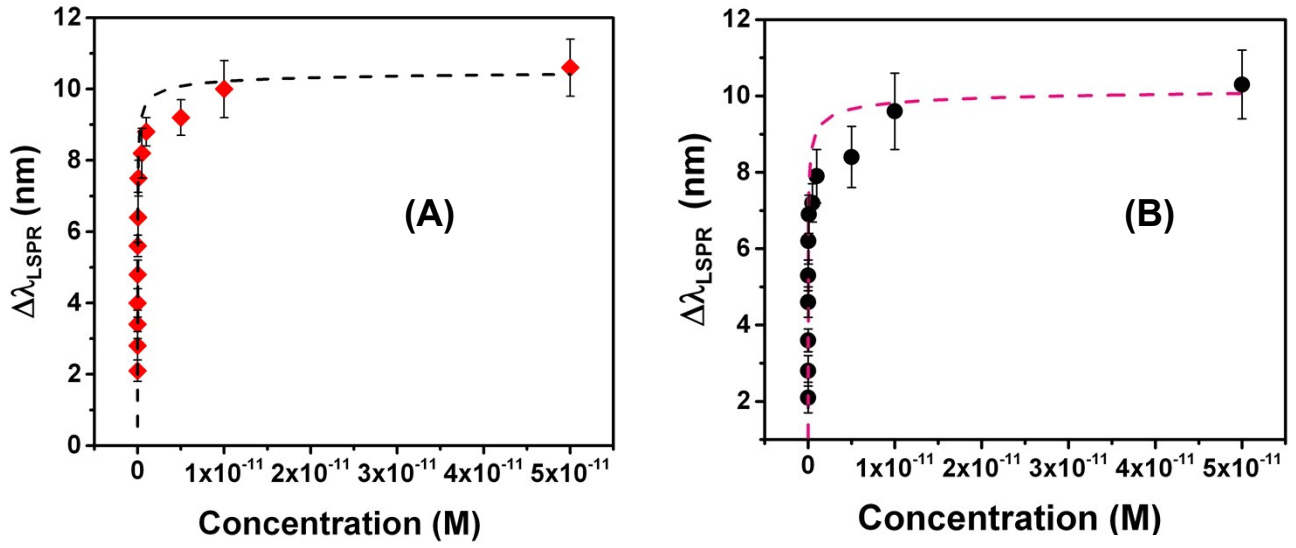

Fig. S7. Binding of chip-based LSPR cTnT sensor in human plasma (A) and human serum (B). The data were fitted to a Langmuir isotherm (dotted line) to determine the K_D values in plasma and serum of 4.25 x10^{-7} and 8.45 x 10^{-7} M, respectively.

Table S7. $\square\lambda_{LSPR}$ responses from chip-based LSPR cTnT sensors fabricated by using MUDA/NT SAM of varied biological fluids. Our current laboratory protocol is to fabricate at least five independent cTnT biosensors (n = 5) from two different batches of Au TNPs to determine the average $\square\lambda_{LSPR}$.

Physiological Media	cTnT Concentration (ng/L)	Average $\square\lambda_{LSPR}$ (nm)	Standard Deviation (nm)
Buffer	1750	11.5	0.7
	350	11.0	0.4
	175	10.1	0.4
	35	9.5	0.5
	17.5	8.8	0.4
	3.5	7.8	0.3
	1.75	7.0	0.3
	0.35	6.0	0.3
	0.175	5.4	0.4
	0.035	4.4	0.4
	0.0175	3.6	0.3
	0.0035	3.0	0.2
	0.00175	2.4	0.2
	0.00035	1.9	0.2
Plasma	1750	10.6	0.8
	350	10	0.8
	175	9.2	0.5
	35	8.8	0.4
	17.5	8.2	0.7
	3.5	7.5	0.5
	1.75	6.4	0.7
	0.35	5.6	0.3
	0.175	4.8	0.4
	0.035	4.0	0.4
	0.0175	3.4	0.4
	0.0035	2.8	0.4
	0.00175	2.1	0.3
Serum	1750	10.3	0.9
	350	9.6	1.0
	175	8.4	0.8
	35	7.9	0.7
	17.5	7.2	0.5
	3.5	6.9	0.5
	1.75	6.2	0.6
	0.35	5.3	0.4
	0.175	4.6	0.4
	0.035	3.6	0.3
	0.0175	2.8	0.4

	0.0035	2.1	0.4
50% Urine	1750	8.5	1.1
	350	8.0	1.3
	175	7.2	1.2
	35	6.2	1.0
	17.5	5.7	0.9
	3.5	4.4	1.1
	1.75	3.3	0.9
	0.35	2.7	0.8
	0.175	2.0	0.8

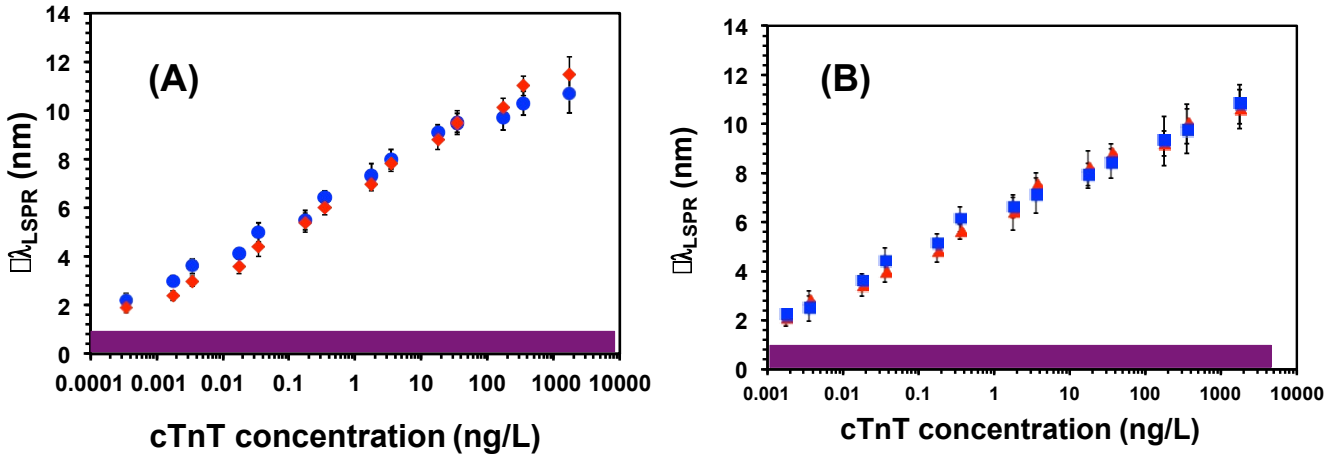

Fig. S8. Reproducibility of the calibration curves in PBS buffer (A) and plasma (B). The purple bar represents three times the standard deviation (σ) of the blank (mixed anti-cTnT/NT functionalized Au TNPs attached onto glass coverslip). (A) Initially constructed sensor (red diamonds) and after 8 months (blue dots). (B) Initially constructed sensor (red triangles) and after 8 months (blue squares).

Discussion Related to Reproducibility: Finally, reproducibility (robustness and consistency of the sensors) is crucial for the design of a reliable cTnT biosensor for point-of-care diagnostics. Our current laboratory protocol is to fabricate at least five independent cTnT biosensors (n = 5) from two different batches of Au TNPs (substrate-to-substrate variation) to determine results such as those described in **Fig. 3, 4A, and 6A**. Moreover, to ensure continued reproducibility of our sensor fabrication, we reconstructed another calibration curve eight month after establishing the first assay and re-determined LODs value in PBS buffer and human plasma (**Fig. S8 and Table S6**). This procedure is very significant in the context of identifying any technical problems that may arise due to batch differences in synthesis materials from suppliers, laboratory temperature variation, etc. Our reproducibility data strongly support the idea of designing chip-based format LSPR cTnT biosensors for point-of-care diagnostics. In order to appropriately develop our detection technique for patient samples, it is crucial to test the self-life (stability of independent cTnT biosensor) of our sensors. Because our cTnT biosensors are constructed on nonreactive glass and the Au TNPs attached onto these substrates are stable, we anticipate our biosensors will have a long shelf life. However, this remains to be demonstrated experimentally and is under investigation.

Table S8. The comparison of detection limit of cTnT by different cTnT sensors.

Method of detection	**LOD**	**Medium**	**Ref.**
Chemiluminescence based - Sandwich ELLISA	8.5 ng/L	Plasma	[7]
Electrochemistry	0.1 ng/L, 0.01ng/L 10 ng/L 1.0 ng/L	Buffer Plasm a Serum	[8] [9] [9] [10]
Photo-electrochemical sensor	20000 ng/L	Buffer	[11]
Electrochem-immunosensor	0.016 ng/L, 16.0 ng/L	Seru m	[12] [13]
Quartz crystal microbalance-immunosensor	5.0 ng/L	Buffer	[14]
Micellar electrokinetic chromatography and a cleavable tag-immunoassay	25 ng/L	Buffer	[15]
Planar nano-gap	0.1 ng/L	Buffer	[16]
LSPR biosensor	**251×10^{-6} ng/L**	**Buffer**	**This article**
	507×10^{-6} ng/L	**Plasma**	**This article**
	766×10^{-6} ng/L	**Serum**	**This article**
	673×10^{-4} ng/L	**Urine**	**This article**

REFERENCES

1 Joshi, G. K.,McClory, P. J.,Muhoberac, B. B.,Kumbhar, A.,Smith, K. A. and Sardar, R. *J. Phys. Chem. C*, 2012, **116**, 20990-21000.

2 Joshi, G. K.,Deitz-McElyea, S.,Johnson, M.,Mali, S.,Korc, M. and Sardar, R. *Nano Lett.*, 2014, **14**, 6955-6963.

3 Joshi, G. K.,Deitz-McElyea, S.,Liyanage, T.,Lawrence, K.,Mali, S.,Sardar, R. and Korc, M. *ACS Nano*, 2015, **9**, 11075-11089.

4 Joshi, G. K.,Blodgett, K. N.,Muhoberac, B. B.,Johnson, M. A.,Smith, K. A. and Sardar, R. *Nano Lett.*, 2014, **14**, 532-540.

5 Marinakos, S. M.,Chen, S. and Chilkoti, A. *Anal. Chem.*, 2007, **79**, 5278-5283.

6 Winter, E. M. and Groves, J. T. *Anal. Chem.*, 2006, **78**, 174-180.

7 Liew, O. W.,Yandle, T. G.,Chong, J. P. C.,Ng, Y. X.,Frampton, C. M.,Ng, T. P.,Lam, C. S. P. and Richards, A. M. *Clin. Chem.*, 2016, **62**, 856-865.

8 Yan, X.-x.,Sun, X.,Niu, A.-j. and Chen, Y.-y. *Yixue Linchuang Yanjiu*, 2015, **32**, 392-394.

9 Liu, Y. and Yobas, L. *Nano Lett.*, 2014, **14**, 6983-6990.

10 Shanmugam, N. R.,Muthukumar, S. and Prasad, S. *Sci. Rep.,* 2016, **6**, 33423.

11 Liu, Y.,Wei, Q.,Ma, H.,Fan, D.,Wang, X.,Hu, L.,Du, B.,Cao, W.,Li, H. and Wu, D. Preparation method and application of Ag2Se@CdSe-labelled sandwiched photoelectrochemical sensor for detection of cardiac troponin T. Application: CN patent 2015-10248843

12 Freitas, T. A.,Mattos, A. B.,Silva, B. V. M. and Dutra, R. F. *BioMed Res. Int.* 2014, 929710.

13 Mattos, A. B.,Freitas, T. A.,Kubota, L. T. and Dutra, R. F. *Biochem. Eng. J.*, 2013, **71**, 97-104.

14 Wong-ek, K.,Chailapakul, O.,Nuntawong, N.,Jaruwongrungsee, K. and Tuantranont, A. *Biomedizinische Technik*, 2010, **55**, 279-284.

15 Caulum, M. M.,Murphy, B. M.,Ramsay, L. M. and Henry, C. S. *Anal. Chem.*, 2007, **79**, 5249-5256.

16 Hsueh, H.-T. and Lin, C.-T. *Biosens. Bioelectron.*, 2016, **79**, 636-643.